12th IFToMM World Congress, Besançon, June 18-21, 2007

Some recent developments in bicycle dynamics

A. L. Schwab*
Lab. for Engineering Mechanics
Delft University of Technology
Mekelweg 2, NL 2628 CD Delft
The Netherlands

J. P. Meijaard†
School of MMME
The University of Nottingham
University Park, Nottingham NG7 2RD
United Kingdom

J. D. G. Kooijman‡
Lab. for Engineering Mechanics
Delft University of Technology
Mekelweg 2, NL 2628 CD Delft
The Netherlands

Abstract—*After more than a century of bicycle dynamics research finally some numerical and experimental validated results on a benchmark bicycle model are available. The phenomenon of self-stability under energy conservation and the controllability of the usually underactuated bicycle are addressed. Some bicycle dynamics folklore is rebutted.*

Keywords: bicycle dynamics, stability, non-holonomic, experiments, benchmark

I. Introduction

The modern bicycle (safety bicycle) as we know it today, was introduced around 1890, having pneumatic tires, a chain drive, a tilted steer axis and front fork offset. Around that time Carvallo [1] and Whipple [2] were the first who used rigid body dynamics analysis to show in theory what was already known in practice: that some bicycles could balance themselves if moving at the right forward speed. From then on scores of people described bicycle dynamics phenomena and/or derived equation of motion for various models and reasons. Few have compared results and most of these do not agree. Finally, Meijaard *et al.* [3] present, as a benchmark, validated linearized equations of motion for a general bicycle model (Whipple) together with a comprehensive literature overview.

In the last decade there has been a swell in bicycle dynamics research. Outstanding contributions, among others, are by Åström, Klein and Lennartsson [4], who present control aspects on a simplified bicycle model, describe decades of experiments on bicycle stability and show some linear and non-linear dynamics observations on a bicycle model developed in a general purpose dynamics code, and by Limebeer and Sharp [5] who present a colourful historical review of various issues associated with bicycle and motorcycle handling, including anecdotes, simple models and complex models.

This paper gives an overview of recent developments in the field of bicycle dynamics. The paper is organized as follows. First, the bicycle model is described. Then the linearized equations of motion for lateral perturbations on the running straight ahead motion are discussed. Then the eigenmotions and stability are presented. In the next section the implications of energy conservation are demonstrated. Then the experimental validation by means of dynamic measurement on an instrumented bicycle is discussed. In the next section the controllability of an underactuated bicycle, with steering torque control only, is investigated. Then an extended bicycle model which compromises finite width tires and propulsion is discussed. Finally some bicycle dynamics folklore is rebutted.

*E-mail: a.l.schwab@tudelft.nl
†E-mail: jaap.meijaard@nottingham.ac.uk
‡E-mail: j.d.g.kooijman@tudelft.nl

II. Bicycle model

The mechanical model of the bicycle [3], [6] consists of four rigid bodies, viz. the rear frame, the front frame being the front fork and handlebar assembly and the two knife-edge wheels. The bodies are interconnected by revolute hinges at the steering head between the rear frame and the front frame and at the two wheel hubs. The rider is assumed to be rigidly connected to the rear frame, hands-free of the handlebar. In the reference configuration, all bodies are assumed to be symmetric relative to the bicycle mid-plane. The contact between the wheels and the flat level

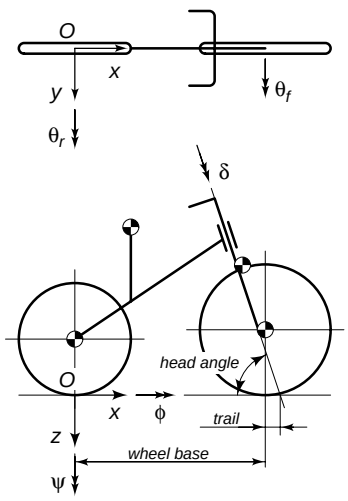

Fig. 1. Bicycle model together with the coordinate system, the degrees of freedom, and the parameters.

surface is modelled as rigid and non-slipping by holonomic constraints in the normal direction and by non-holonomic

Parameter	Symbol	Value
Wheel base	w	1.02 m
Trail	t	0.08 m
Head angle	α	$2\pi/5$ rad
Gravity	g	9.81 N/kg
Forward speed	v	*variable* m/s
Rear wheel		
Radius	R_{rw}	0.3 m
Mass	m_{rw}	2 kg
Mass moments of inertia	(A_{xx}, A_{yy}, A_{zz})	$(0.0603, 0.12, 0.0603)$ kgm^2
Rear frame		
Position centre of mass	(x_{rf}, y_{rf}, z_{rf})	$(0.3, 0, -0.9)$ m
Mass	m_{rf}	85 kg
Mass moments of inertia	$\begin{bmatrix} B_{xx} & 0 & B_{xz} \\ & B_{yy} & 0 \\ sym. & & B_{zz} \end{bmatrix}$	$\begin{bmatrix} 9.2 & 0 & 2.4 \\ & 11 & 0 \\ & & 2.8 \end{bmatrix}$ kgm^2
Front frame		
Position centre of mass	(x_{ff}, y_{ff}, z_{ff})	$(0.9, 0, -0.7)$ m
Mass	m_{ff}	4 kg
Mass moments of inertia	$\begin{bmatrix} C_{xx} & 0 & C_{xz} \\ & C_{yy} & 0 \\ sym. & & C_{zz} \end{bmatrix}$	$\begin{bmatrix} 0.05892 & 0 & -0.00756 \\ & 0.06 & 0 \\ & & 0.00708 \end{bmatrix}$ kgm^2
Front wheel		
Radius	R_{fw}	0.35 m
Mass	m_{fw}	3 kg
Mass moments of inertia	(D_{xx}, D_{yy}, D_{zz})	$(0.1405, 0.28, 0.1405)$ kgm^2

TABLE I. Parameters for the benchmark bicycle depicted in figure 1 and described in the text. The values given are exact (no round-off).

constraints in the longitudinal and lateral directions. It is assumed that there is no friction, apart from the idealized friction between the non-slipping wheels and the surface, and no propulsion. These assumptions make the model energy-conserving. Figure 1 shows the bicycle model in the reference configuration.

The mechanical model of the bicycle has three velocity degrees of freedom: the roll rate $\dot{\phi}$ of the rear frame, the steering rate $\dot{\delta}$, and the angular rate $\dot{\theta}_r$ of the rear wheel with respect to the rear frame. Due to the non-holonomic constraints there are four extra so-called kinematic coordinates which describe, together with the degrees of freedom, the configuration of the system [7]. For example, the bicycle can move sideways by the same motions used to parallel-park a car. The four kinematic coordinates are taken here as the Cartesian coordinates x and y of the rear-wheel contact point, the yaw angle ψ of the rear frame, and the rotation θ_f of the front wheel with respect to the front frame. The design for this bicycle model is fully described by 25 geometric and mass parameters, such as wheelbase, trail and head angle. Table I lists these parameters and the gravity together with the numerical values used for the benchmark bicycle [3].

III. Equations of motion

Here we present the linearized equations of motion for a bicycle slightly perturbed from running upright straight-ahead at a steady forward speed. The lateral symmetry of the system, combined with the linearity in the equations, precludes any coupling between the forward motion and the lean and steer. Therefore the first linearized equation of motion is $\ddot{\theta}_r = 0$. Consequently the nominal forward speed $v = -\dot{\theta}_r R_{rw}$ is constant.

The linearized equations of motion for the bicycle expressed in the two remaining degrees of freedom, the lean angle ϕ and the steer angle δ, are two coupled second-order constant-coefficient ordinary differential equations with the forward speed as a parameter. The first equation is called *the lean equation* and the second is called *the steer equation*. Written in matrix form we have [3], [6]:

$$\mathbf{M}\ddot{\mathbf{q}} + [v\mathbf{C}_1]\dot{\mathbf{q}} + [g\mathbf{K}_0 + v^2\mathbf{K}_2]\mathbf{q} = \mathbf{f}, \qquad (1)$$

where the time-varying variables are $\mathbf{q} = [\phi, \delta]^T$ and the forcing $\mathbf{f} = [T_\phi, T_\delta]^T$. The constant entries in matrices $\mathbf{M}$, $\mathbf{C}_1$, $\mathbf{K}_0$ and $\mathbf{K}_2$ are complex expressions in terms of the 25 design parameters, and can be found in [6]. Briefly, $\mathbf{M}$ is a symmetric mass matrix which gives the kinetic energy of the bicycle system at zero forward speed by $\dot{\mathbf{q}}^T\mathbf{M}\dot{\mathbf{q}}/2$. The damping-like (there is no real damping) matrix $v\mathbf{C}_1$ is linear in the forward speed v and captures gyroscopic torques due to steer and lean rate, inertial reaction from the rear frame yaw rate (due to trail), and from a reaction to yaw acceleration proportional to steer rate. The stiffness matrix is the sum of two parts: a velocity-independent symmetric part $g\mathbf{K}_0$ proportional to the gravitational acceleration, which can be used to calculate changes in potential energy with $\mathbf{q}^T[g\mathbf{K}_0]\mathbf{q}/2$, and a part $v^2\mathbf{K}_2$ which is quadratic in the forward speed and is due to gyroscopic and centrifugal effects. To get an idea about the structure of these equations we present for the benchmark bicycle (table I) the values of the entries in the matrices as:

$$\mathbf{M} = \begin{bmatrix} 80.817, & 2.319 \\ 2.319, & 0.298 \end{bmatrix}, \quad \mathbf{C1} = \begin{bmatrix} 0, & 33.866 \\ -0.850, & 1.685 \end{bmatrix},$$
$$\mathbf{K0} = \begin{bmatrix} -80.95\ , & -2.600 \\ -2.600, & -0.803 \end{bmatrix}, \qquad \mathbf{K2} = \begin{bmatrix} 0, & 76.597 \\ 0, & 2.654 \end{bmatrix}. \qquad (2)$$

These values are rounded off but an essential zero is written as 0.

IV. Stability and eigenmotions

The stability of the the upright straight-ahead running solution at constant forward speed v can be found by investigating the eigenvalues of the system. Moreover, transient response of the system, in the absence of any forcing, is given by a linear combination of the corresponding eigenmodes. These eigenmodes together with their eigenvalues are found by assuming an exponential solution of the form $\mathbf{q} = \mathbf{q_0}\exp(\lambda\mathbf{t})$ for the homogeneous equations from (1). This leads to a characteristic polynomial which is quartic in λ. The coefficients in this polynomial are complex expressions of the 25 design parameters, gravity, and speed v. The solutions λ of the characteristic polynomial for a range of forward speeds are shown in figure 2. Eigenvalues with a positive real part correspond to unstable motions whereas eigenvalues with a negative real part correspond to asymptotically stable motions for the corresponding mode. Imaginary eigenvalues correspond to oscillatory motions.

In principle there are up to four eigenmodes, where oscillatory eigenmodes come in pairs. Two are significant and are traditionally called the *capsize mode* and *weave mode*. The capsize mode corresponds to a real eigenvalue with

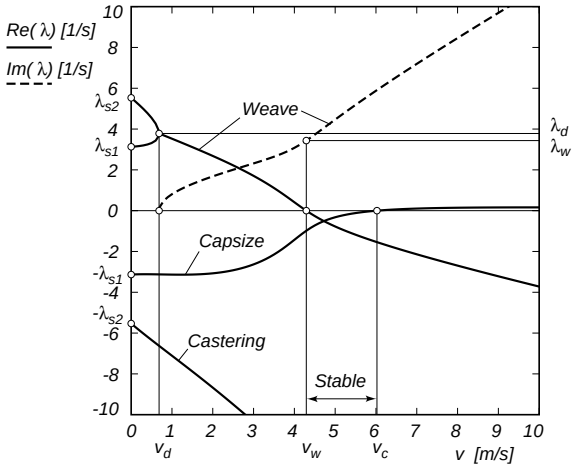

Fig. 2. Eigenvalues λ from the linearized stability analysis for the benchmark bicycle from figure 1 and table I where the solid lines correspond to the real part of the eigenvalues and the dashed line corresponds to the imaginary part of the eigenvalues, in the forward speed range of $0 \leq v \leq 10$ m/s. The speed range for the asymptotic stability of the benchmark bicycle is $v_{\mathrm{w}} < v < v_{\mathrm{c}}$. The zero crossings of the real part of the eigenvalues are for the weave motion at the weave speed $v_{\mathrm{w}} \approx 4.292\,\mathrm{m/s}$ and for the capsize motion at capsize speed $v_{\mathrm{c}} \approx 6.024\,\mathrm{m/s}$, and there is a double real root at $v_{\mathrm{d}} \approx 0.684\,\mathrm{m/s}$.

eigenvector dominated by lean: when unstable, the bicycle just falls over like a capsizing ship. The weave mode is an oscillatory motion in which the bicycle sways about the headed direction. The third remaining eigenmode is the *caster mode* which corresponds to a large negative real eigenvalue with eigenvector dominated by steering.

At near-zero speeds, typically $0 < v < 0.5$ m/s, there are two pairs of real eigenvalues. Each pair consists of a positive and a negative eigenvalue and corresponds to an inverted-pendulum-like falling of the bicycle. Then at $v_d \approx 0.684$ m/s two real eigenvalues become identical and form a complex conjugate pair; this is where the oscillatory weave motion emerges. At first this motion is unstable but at $v_w \approx 4.292$ m/s, the weave speed, these eigenvalues cross the imaginary axis in a Hopf bifurcation and this mode becomes stable. At high speeds the frequency of the weave motion is approximately proportional to the forward speed, meaning that the wavelength of the oscillation becomes constant. Meanwhile the capsize motion, which was stable for low speed, crosses the real axis in a pitchfork bifurcation at $v_c \approx 7.896$ m/s, the capsize speed, and the motion becomes mildly unstable. With further increase in speed, the unstable capsize eigenvalue approaches zero (from above). The speed range for which the uncontrolled bicycle shows asymptotically stable behaviour is $v_w < v < v_c$. In summary, at low speed (below the weave speed) the bicycle is in need of control whereas at higher speeds the bicycle is either self-stable or easy to stabilize.

V. Energy conservation

When an uncontrolled bicycle is within its stable speed range, roll and steer perturbations die away in a seemingly damped fashion. However, the system conserves energy. As the forward speed is affected only to second order, linearized equations do not capture this energy conservation. Therefore a non-linear dynamic analysis with the multibody dynamics code SPACAR [8], [7] was performed on the benchmark bicycle model to demonstrate the loss of energy from lateral perturbations into forward speed. The initial conditions at $t = 0$ are the upright reference position at a forward speed of $v = 4.6$ m/s, which is within the stable speed range of the linearized analysis, and an initial angular roll velocity of $\dot{\phi} = 0.5$ rad/s.

Figure 3 shows the transient response of the non-linear system. There is a small increase of about 0.022 m/s in the forward speed v while the lateral motions die out, as expected. The final upright forward speed is augmented from the initial speed by an amount determined by the energy in the lateral perturbation. The same figure also shows that

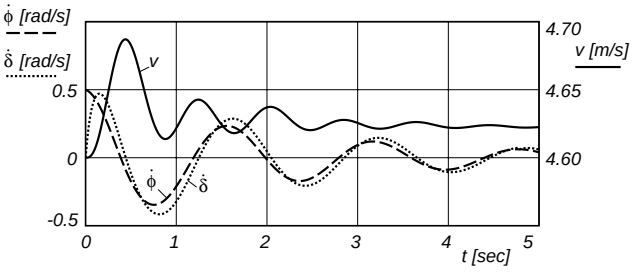

Fig. 3. Non-linear dynamic response of the benchmark bicycle from figure 1 and table I, with the angular roll velocity $\dot{\phi}$, the angular steering velocity $\dot{\delta}$, and the forward speed $v = -R_{rw}\dot{\theta}_r$ for the initial conditions: $(\phi, \delta, \theta_r)_0 = (0, 0, 0)$ and $(\dot{\phi}, \dot{\delta}, v)_0 = (0.5\ \mathrm{rad/s}, 0, 4.6\ \mathrm{m/s})$ for a time period of 5 seconds.

the period for the roll and steer oscillations is approximately $T_0 = 1.60$ s, which compares well with the 1.622 s from the linearized stability analysis. The lack of agreement in the second decimal place is from finite-amplitude effects, not numerical accuracy issues. When the initial lateral velocity is decreased by a factor of 10 the period of motion matches the linear prediction to 4 digits. The steering motion $\dot{\delta}$ has a small phase lag relative to the roll motion $\dot{\phi}$ visible in the solution in figure 3.

VI. Experimental validation

In the bicycle model, many physical aspects of the real bicycle are considered negligible, such as the flexibility of the frame and wheels, play in the bearings, and tire deformation and slip. The admissibility of these assumptions can be checked by comparing experimental results with numerical simulation results [9]. The experimental system consists of an instrumented bicycle without rider, see Figure 4. Sensors are present for measuring the roll rate and the yaw rate,

Fig. 4. Instrumented bicycle with all the measurement equipment installed. Sensors are present for measuring the roll rate, yaw rate, steering angle, and rear wheel rotation. Data is collected via a USB-connected data acquisition unit on the laptop computer, mounted on the rear rack.

the steering angle and the rear wheel rotation. The data are collected on a laptop computer mounted on the rear rack. Trainer wheels prevent the complete fall of the bicycle for unstable conditions.

Measurements are recorded for the case in which the bicycle is manually launched and coasts freely on a level surface. To measure the dynamic response of the bicycle at different speeds the bicycle has to show some lateral dynamics. At speeds below the stable speed range no external excitation is required; small asymmetry or non perfect initial conditions always initiate the unstable lateral dynamics. For runs in the stable speed range the bicycle is excited by applying manually a lateral impulse to the bicycle. For a bicycle of the usual construction the principal transient motion within the speed range of 2 to 6 m/s (manual launch) is the weave motion. The stable capsize and caster mode die out fast and are indiscernible. Then, from the measured data, eigenvalues are extracted by fitting a growing or decaying oscillating weave motion to the measured data.

The results from a total of 76 runs are presented in Figure 5. During the measurement the forward speed will slightly decrease. Therefore the results are presented within a forward speed range (horizontal bars) instead of at a fixed speed. The continuous lines represent the eigenvalues as obtained from the linearized analysis on the bicycle model (measuring the 25 design parameters of the instrumented bicycle for this model turned out to be a project in itself [9]). The experimental results show a very good agreement with the results as obtained by a linearized analysis on the three degrees-of-freedom model of the bicycle. This shows that the tire slip and frame and fork compliance are not important for the lateral dynamics of the bicycle in the forward speed range from 2 to 6 m/s.

VII. Controllability

From the linearized stability analysis (Section III) and from experience, it is clear that some rider control is needed to ride a bicycle in a stable manner. In particular at low speed, that is beneath the weave speed, when the system

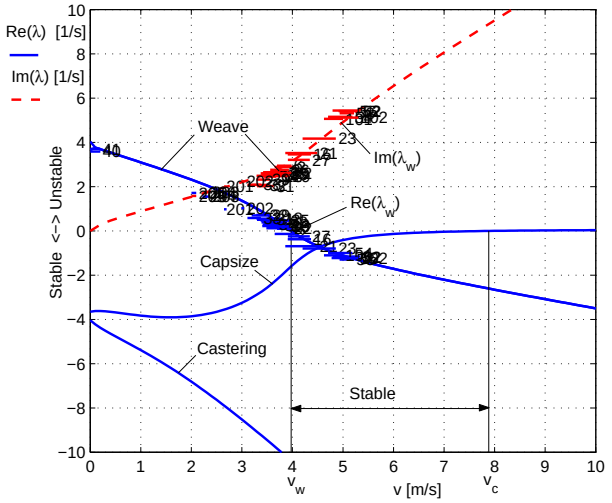

Fig. 5. Measured eigenvalues λ (horizontal bars) and calculated eigenvalues λ (continuous lines) for the instrumented bicycle from figure 4, in the forward speed range of $0 \leq v \leq 10$ m/s. For the measured values only the weave motion is considered. The length of the horizontal bars indicate the forward speed range during the measurement, numbers indicate the corresponding test run. For the calculated values the solid lines correspond to the real part of the eigenvalues and the dashed line corresponds to the imaginary part of the eigenvalues. The zero crossings of the real part of the eigenvalues are for the weave motion at the weave speed $v_w \approx 4.0$ m/s and for the capsize motion at capsize speed $v_c \approx 7.9$ m/s. The speed range for the asymptotic stability of the instrumented bicycle is $v_w < v < v_c$.

is highly unstable (see Figure 2). Indeed, riding a bicycle is an acquired skill. Above the capsize speed the system becomes mildly unstable (eigenvalue positive, but small) and stabilizing is fairly easy. Seffen *et al.* [10] are among the few who investigate the controllability of a bicycle.

In normal operation, control actions are preformed by both body lean and steering torque. However, the steering torque influence appears to be dominant [11]. Therefore, we will consider a system only controlled by steering torque. The question arises if such an underactuated system can be controlled at any forward speed. To investigate this controllability we rewrite the linearized equations of motion (1) into a set of first order differential equations, the so-called state-space form

$$\dot{\mathbf{x}} = \mathbf{A}\mathbf{x} + \mathbf{B}\mathbf{u}, \tag{3}$$

where the state vector is $\mathbf{x} = [\phi, \delta, \dot{\phi}, \dot{\delta}]^T$ and the control input vector $\mathbf{u} = [T_\delta]$. The coefficient matrices $\mathbf{A}$ and $\mathbf{B}$ are given by

$$\mathbf{A} = \begin{bmatrix} \mathbf{0} & \mathbf{I} \\ -\mathbf{M}^{-1}(\mathbf{K}_0 + v^2\mathbf{K}_2) & -\mathbf{M}^{-1}(v\mathbf{C}_1) \end{bmatrix}, \tag{4}$$

$$\mathbf{B} = \begin{bmatrix} \mathbf{0} \\ \mathbf{M}^{-1}[0,1]^T \end{bmatrix}. \tag{5}$$

The system is completely controllable if the matrix

$$\mathbf{Q} = [\mathbf{B}, \mathbf{A}\mathbf{B}, \mathbf{A}^2\mathbf{B}, \cdots, \mathbf{A}^{k-1}\mathbf{B}], \tag{6}$$

has full rank k, where k is the order of the system and equal to the number of states. Here, we investigate rank deficiency by setting the determinant of $\mathbf{Q}$ to zero. This leads to a characteristic equation in the forward speed v, since the speed is a parameter. For the bicycle model this equation turns out to be quadratic in v^2 so we can have at the most two forward speeds for which the system is uncontrollable. Substitution of the matrix values from the benchmark bicycle (2) and solving for v leads to two real and positive velocities $v_1 = 0.025$ and $v_2 = 1.411$ m/s for which the system is uncontrollable. The corresponding system eigenvalues are equal and opposite: $\lambda_1 = 3.135$ and $\lambda_2 = -3.135$ rad/s. The positive eigenvalue corresponds to the unstable pendulum-like motion and the negative eigenvalue to the stable capsize motion, see Figure 2. Since the capsize is already stable we conclude that the benchmark bicycle, controlled only by a steering torque, is uncontrollable at $v_1 = 0.025$ m/s. This speed is almost zero and therefore, from a practical point of view, we conclude that the underactuated benchmark bicycle can be fully controlled by only steering torque; indeed, a thing most of us know from experience.

VIII. Extended bicycle model

The bicycle model from section II can be extended in several ways, while the simplicity of having only two degrees of freedom, lean and steer, is retained [12]. A first extension to the model is the finite transverse radius of curvature of the crown of the wheel. Without loss of generality for the linearized equations, the outer shape of the wheel tire is considered to be toroidal, see Figure 6. The contact between the tire and the road is in a single point, which has a vanishing velocity, so two non-holonomic constraints are imposed for the longitudinal and lateral slip velocities. The position of the contact point is in the vertical plane through the centre of the wheel at an angle at the crown radius that is equal to the inclination angle of the wheel. A second extension considers the accelerated bicycle. The acceleration can be caused by a road gradient, by moments at the hubs of the rear and front wheel and by aerodynamic drag.

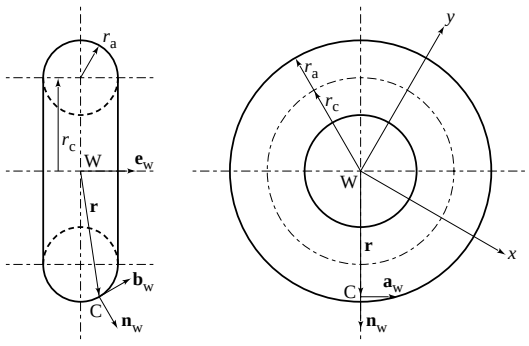

Fig. 6. Toroidal shaped wheel with point of contact C and outer surface normal n_w.

The effect on the linearized equations of motion is as follows. The first equation, forward speed, is only affected in the right-hand side by extra forcing terms from gravity on a slope f_g , moments at the hub f_m and the aerodynamic drag f_d, and takes on the form:

$$m_e \dot{v} = f_g + f_m + f_d, \tag{7}$$

where m_e is the effective mass of the system which contains contributions due to the moments of inertia of the wheels.

Owing to the gradient, the yaw angle of the rear frame is no longer a cyclic coordinate and the kinematic differential equation for its evolution needs to be included. The linearized equations of motion for lean and steer now take on the follow form:

$$\mathbf{M}\ddot{\mathbf{q}} + [v\overline{\mathbf{C}}_1]\dot{\mathbf{q}} + [\overline{\mathbf{K}}_0 + \dot{v}\mathbf{K}_1 + v^2\overline{\mathbf{K}}_2]\mathbf{q} + \mathbf{K}^k\mathbf{q}^k = \mathbf{f}, \tag{8}$$

where the time-varying variables are the degrees of freedom $\mathbf{q} = [\phi, \delta]^T$, the non-cyclic kinematic coordinate $\mathbf{q}^k = [\psi]$ and the additional forcing terms $\mathbf{f} = [T_\phi, T_\delta]^T$.

The symmetric mass matrix $\mathbf{M}$ is unaltered compared to (1). The damping-like coefficient matrix $\overline{\mathbf{C}}_1$ shows some additional terms due to the aerodynamic drag, which give damping on the lean angle.

The finite transverse tire radius only modifies the constant part of the stiffness matrix $\overline{\mathbf{K}}_0$ (which is now no longer symmetric), and indirectly, through the drag, the part that is proportional to the square of the velocity $\overline{\mathbf{K}}_2$. Because the contact point shifts in lateral direction if the bicycle rolls, the capsize instability is reduced in strength.

The longitudinal forces that contribute to the acceleration of the bicycle have a contribution that is common to that of a driving torque at the rear wheel and which is described by the matrix $\mathbf{K}_1$, and some additional influences. This shows that the way in which the bicycle is accelerated or decelerated has an influence on the lateral dynamics. Moreover, driving the bicycle at the rear wheel and simultaneously braking at the front wheel to keep the speed constant can improve the stability. This effect is represented by terms in $\overline{\mathbf{K}}_0$.

In the presence of a gradient, the matrix $\mathbf{K}^k$ describes the additional stiffness due to the non-cyclic yaw angle. In this case the neutral stability of the bicycle is lost: it has either a weak directional stability or a weak directional instability. In most cases, it has a tendency to steer towards the downhill direction, which means that riding down a slope leads to directional stability and riding up a slope leads to directional instability. Effects on the other eigenmodes are generally more important, however.

IX. Folklore

The world of bicycle dynamics is filled with folklore. For instance, some publications persist in the necessity of positive trail or gyroscopic effect of the wheels for the existence

of a forward speed range with uncontrolled stable operation. Here we will show, by means of a counter example, that this is not necessarily the case.

Consider the bicycle model from Section II but with the following dimensions and mechanical properties. The wheel base is 1.2 m at zero trail, and the head angle is 85 degrees. Both wheels are massless and have a diameter of 0.35 m. The mass distribution of the rear frame is modelled by two point masses, one of 40 kg upfront at $(x, z) = (1.5, -0.6)$ m and one of 40 kg at the rear contact point. The latter has to insure contact at the rear wheel, but gives no contribution to the linearized equations of motion. The front fork has a mass of 1 kg located at front hub, $(x, z) = (1.2, -0.35)$ m and zero mass moment of inertia. Gravity is 9.81 N/kg. In short, this resembles a bicycle on skates (no rotating wheels) with the centre of mass of the rear frame forward and a very light zero-trail steering assembly.

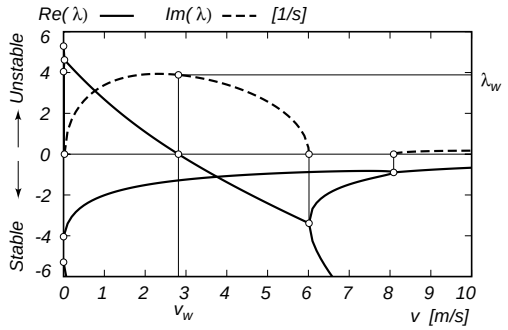

Fig. 7. Eigenvalues λ from the linearized stability analysis for a bicycle with zero trail and no gyroscopic effects from Section IX. The solid lines correspond to the real part of the eigenvalues and the dashed line corresponds to the imaginary part of the eigenvalues, in the forward speed range of $0 \leq v \leq 10$ m/s. The zero crossing of the real part of the eigenvalues is for the weave motion at the weave speed $v_w \approx 4.302$ m/s and there are three double real roots at $v \approx 0.022$, 6.014, and 8.089 m/s. The asymptotically stable speed range for this bicycle is $v_w < v < \infty$.

The stability analysis on the forward upright motion of this model results in a weave speed $v_w = 2.815$ m/s and no capsize speed, see Figure 7. Inspection of the eigenvalues for a wide forward speed range shows that the capsize motion is always stable and that *all* eigenvalues above the weave speed have a negative real part. In other words, this bicycle with zero trail and zero gyroscopic effect shows asymptotically stable uncontrolled motion for the broad forward speed range of $2.815 \leq v \leq \infty$ m/s.

X. Closure

Several aspects of the three degrees-of-freedom bicycle model have been demonstrated, some based on the now well established linearized equations of motion. However, this still does not address the question "How does an uncontrolled bicycle stay up?". Therefore future work will be directed to address how self-stability does and does not depend on the bicycle design parameters. Another line of research will be devoted to investigating the way a human controller stabilizes a bicycle during normal and emergency operation and finally to understand and define the concept of bicycle handling qualities.

Acknowledgements

We thank A. Ruina, J. M. Papadopoulos and A. Dressel for the close collaboration, extensive discussions and technical comments.

References

[1] Carvallo, E. (awarded Prix Fourneyron 1898, submitted 1897). Also published as Théorie du mouvement du Monocycle et de la Bicyclette. *Journal de L'École Polytechnique*, Series 2, Part 1, Volume 5, "Cerceau et Monocyle", pp. 119–188, 1900. Part 2, Volume 6, "Théorie de la Bicyclette", pp. 1–118, 1901.

[2] Whipple, F. J. W. The Stability of the Motion of a Bicycle. *The Quarterly Journal of Pure and Applied Mathematics* **30**:312–348, 1899.

[3] Meijaard, J. P., Papadopoulos, J. M., Ruina, A. and Schwab, A. L. Linearized dynamics equations for the balance and steer of a bicycle: a benchmark and review. Submitted to *Proceedings of the Royal Society A* (Oct. 2006).

[4] Åström, K.J., Klein, R.E. and Lennartsson, A. Bicycle dynamics and control: Adapted bicycles for education and research. *IEEE Control Systems Magazine* **25**(4):26–47, 2005.

[5] Limebeer, D. J. N. and Sharp, R. S. Bicycles, motorcycles, and models, *IEEE Control Systems Magazine* **26**(5):34–61, 2006

[6] Schwab, A. L., Meijaard, J. P. and Papadopoulos, J. M. Benchmark results on the linearized equations of motion of an uncontrolled bicycle. *KSME International Journal of Mechanical Science and Technology* **19**(1):292–304, 2005.

[7] Schwab, A. L. and Meijaard, J. P. Dynamics of flexible multibody systems with non-holonomic constraints: A finite element approach. *Multibody System Dynamics* **10**:107–123, 2003.

[8] Jonker, J. B. and Meijaard, J. P. SPACAR—Computer program for dynamic analysis of flexible spatial mechanisms and manipulators. In *Multibody Systems Handbook* (ed. W. Schiehlen). Berlin: Springer-Verlag, pp. 123–143, 1990.

[9] Kooijman, J. D. G. Experimental Validation of a Model for the Motion of an Uncontrolled Bicycle, M.Sc. thesis, Delft University of Technology, April 2006.

[10] Seffen, K.A., Parks, G.T. and Clarkson P.J. Observations on the controllability of motion of two-wheelers, *Proceedings of the Institution of Mechanical Engineers, Part I Systems and Control Engineering* **215**(12):143–156, 2001.

[11] Weir, D. H. and Zellner, J. W. Lateral-directional motorcycle dynamics and rider control. Technical report no. 780304, Society of Automotive Engineers, Warrendale, PA, 1978.

[12] Meijaard, J. P. and Schwab, A. L. Linearized Equations for an Extended Bicycle Model, C.A. Mota Soares et al. eds. *III European Conference on Computational Mechanics Solids, Structures and Coupled Problems in Engineering*, 18 pp., Lisbon, Portugal, 5–9 June 2006.

[13] Schwab, A. L. , Meijaard, J. P. and Kooijman, J. D. G. Experimental validation of a model of an uncontrolled bicycle, C.A. Mota Soares et al. eds. *III European Conference on Computational Mechanics Solids, Structures and Coupled Problems in Engineering*, 16 pp., Lisbon, Portugal, 5–9 June 2006.